Loughborough University

This item was submitted to Loughborough's Research Repository by the author.
Items in Figshare are protected by copyright, with all rights reserved, unless otherwise indicated.

Simulation platform for autonomous smart multi-terminal DC micro-grid

PLEASE CITE THE PUBLISHED VERSION

http://dx.doi.org/10.1109/ISGT-Asia.2016.7796458

PUBLISHER

© IEEE

VERSION

AM (Accepted Manuscript)

PUBLISHER STATEMENT

© 2016 IEEE. Personal use of this material is permitted. Permission from IEEE must be obtained for all other uses, in any current or future media, including reprinting/republishing this material for advertising or promotional purposes, creating new collective works, for resale or redistribution to servers or lists, or reuse of any copyrighted component of this work in other works.

LICENCE

All Rights Reserved

REPOSITORY RECORD

Gonzalez-Longatt, Francisco, Bharat Singh Rajpurohit, J.L. Rueda Torres, and Sri Niwas Singh. 2019. “Simulation Platform for Autonomous Smart Multi-terminal DC Micro-grid”. figshare. https://hdl.handle.net/2134/24269.

Simulation Platform for Autonomous Smart Multi-terminal DC Micro-Grid

F. Gonzalez-Longatt
Electronic, Electrical and Systems Engineering School
Loughborough University
Loughborough, UK
fglongatt@fglongatt.org

B. S. Rajpurohit
School of Computing & Electrical Engineering
IIT Mandi,
Mandi, India
bsr@iitmandi.ac.in

J.L. Rueda Torres
Department of Electrical Sustainable Energy, Delft University of Technology
Delft, Netherlands
j.l.ruedatorres@tudelft.nl

S.N. Singh
Electrical Engineering Department
IIT Kanpur
Kanpur India
snsingh@iitk.ac.in

***Abstract*—This paper presents a compressive introduction to the development of a simulation platform for smart multi-terminal DC micro-grid (sMTdc), this tool will facilitate the development of DC network to support a low-carbon sustainable electricity supply system. The simulation platform uses a compressive set of high-resolution (1-min) sub-models: generation (photovoltaic, wind power), demand (individual appliances) and battery energy storage system (BESS). A *Quasi-dynamic* simulation approach using *optimal power flow* (OPF) to minimize the system losses is used to obtain the voltage profile, power losses and state of charge of the BESS. The simulation platform has been used to shows the performance of an illustrative/demonstrative sMTdc based on 3 DC-Houses.**

***Keywords*— DC-grids, electrical energy storage, microgrids, optimization, renewable energy sources.**

I. INTRODUCTION

Looking to the future, there are several challenges that the electricity networks will face: prosperity, sustainable growth global and security. The electricity industry situation is complex because resources across the world are becoming scarce and the need for sustainable growth is increasingly important [1]. Now, the evolution of a *decarbonised economy* involves three main aspects [1]: (i) developing *energy efficiency* measures, (ii) developing *renewable energy* capabilities and (iii) to deal with adaptation needs arising due to *climate change*. Energy efficiency is one of the key factors on migrating to a decarbonised economy, i.e. moving to a low-carbon society. *European Union* (EU) is expecting to use around 30% less energy in 2050 than in 2005 [2]. A decarbonised society involves people living and working in low-energy, low-emission buildings, including intelligent heating and cooling systems, and other low energy and high-efficiency energy services (transportation, etc.).

The transition to a low carbon economy provides huge opportunities to improve the energy use of both domestic and business customers. Households and businesses would take advantage of more secure and efficient energy including two important benefits [2]: reducing energy bills while at the same time, delivering a more sustainable society. Several initiatives around the world are working on the development of *very low energy buildings* [3-8].

In March 2014, a consortium of UK and Indian universities was generated: Loughborough University from the UK side and Indian Institute of Technology (IIT) Mandi and IIT Kanpur, from the Indian side [9]. The consortium has been working on a research project named "*Smart Multi-Terminal DC μ-grids for autonomous Zero-Net-Energy Buildings*" (DST/INT/UK/P-61/2014). The research project is indented to creating a *smart multi-terminal DC micro-grid* (sMTdc) to enable the development of autonomous zero net energy building [10].

This paper presents a compressive introduction to the development of a simulation platform for smart multi-terminal DC micro-grid, this tool will facilitate the development of DC network to support a low-carbon sustainable electricity supply system. The rest of the paper is structured in the following sequence: Section II presents the general architecture of the *smart multi-terminal DC micro-grid* (sMTdc) and the model the main components are presented on Section III. Section IV introduces the concept of "*Quasi-dynamic*" simulation used in this paper to evaluate the performance of the sMTdc. Simulation and results are shown in Section V and conclusions are discussed in Section VI.

II. MICRO-GRID ARCHITECTURE

The classical concept of microgrid (μg) consists of interconnected *distributed energy resources* (DER) capable of providing sufficient and continuous energy to a significant portion of internal load demand. The μg concept has been extraordinary explored in the literature, especially the connection to the traditional AC system. However, the project "*Smart Multi-Terminal DC μ-grids for autonomous Zero-Net-Energy Buildings*" requires a special vision the μg considering it as an *autonomous system*. It means the μg is designed to be operated independently from any ac infrastructural support. In this paper, the *smart multi-terminal DC micro-grid* (sMTdc) consist of two sub-structures: (i) DC nano-grid and (ii) DC micro-grid.

A. DC nano-grid

The DC nano-grid (n-g), as its name indicates, a very small version of a microgrid, it is used as electrical infrastructure serving a single *DC-House*. Fig. 3 presents a schematic representation of a generic n-g used to distribute the electricity

inside a DC-House, several components of the n-g are depicted: *power generation* (PV and wind power) and *local demand* (dump loads and variable load). It should be noticed there is not *electrical energy storage* (EES) included in this model.

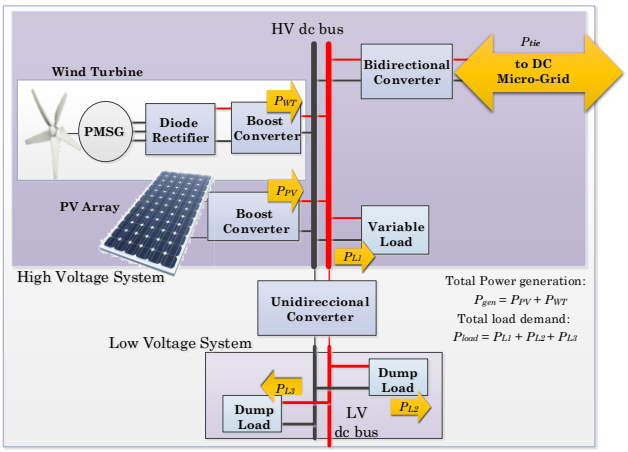


Fig. 1. Schematic diagram of a DCNano-grid representing a DC-House.

B. *DC micro-grid*

The DC multi-terminal DC grid is the high power layer, which is used to interconnect several DC-houses (n-g), and this grid is there all the major energy interaction between n-gs happen. The DC micro-grid is the core of the *smart multi-terminal DC micro-grid* (sMTdc). A communal *battery energy storage system* (BESS) is included in the sMTdc in order to enhance the energy security. Interactions between generation-demand-storage are one of the key components of sMTdc (see Fig. 2).

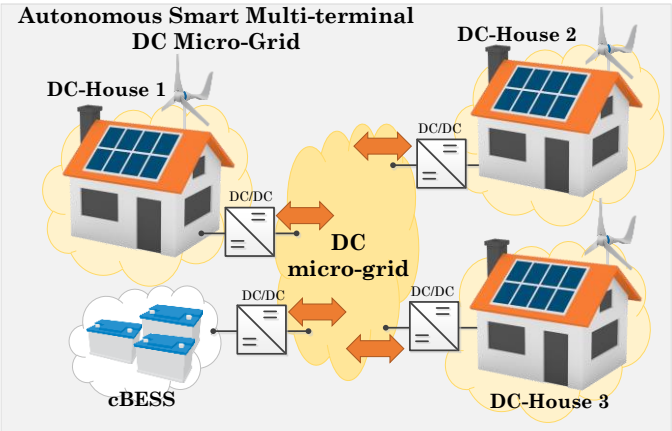


Fig. 2. Schematic diagram of a DC micro-grid representing a DC community.

III. Model Architecture of DC-House

Energy use in the DC-home is a major source electricity consumption and is highly dependent on the activities of the residents [10, 11]. An adequate simulation model of the electricity demand inside a DC-House must be able of reflects dependent upon the activities of the occupants and their associated use of electrical appliances. In this paper, a *high-resolution model of domestic electricity use* is used. It is based on a combination of patterns of *active occupancy* [12].

The original model of the high-resolution model of domestic electric used was introduced by I. Richardson et al. in [13], and several improvements have been developed during years [14-16]. The construction and validation of this model are presented in earlier published work by the I Richardson. In this paper, the high-resolution model has been modified and improved including wind power generation. A general overview of the DC-House model is depicted in Fig. 3.

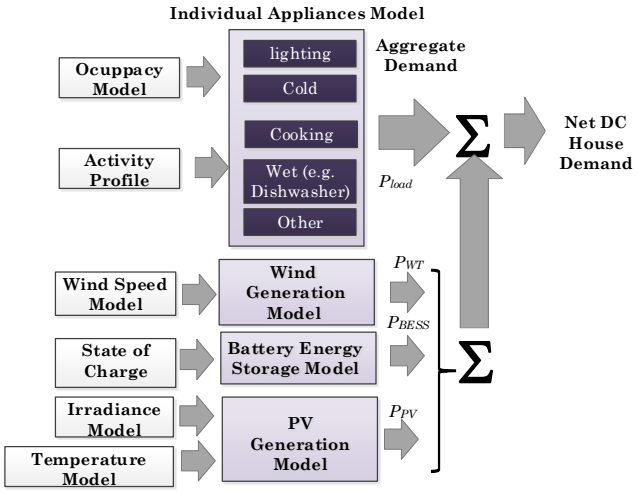


Fig. 3. Outline Structure of the High-Resolution Model of DC-House.

The outdoor irradiance, outdoor temperature, and wind speed are used as inputs to the model. The core of this model includes the simulation of the major types of domestic electrical appliances, including cold, cooking, and wet categories. The active occupancy as a main component of the model in order to introduce the social behaviour influencing the domestic energy demand. The following subsection defines the main subcomponents of the model.

A. *Active domestic occupancy model*

The *model of active domestic occupancy* defines the numbers of occupants that are within the DC-house, and this is a key element because it is identified to be a main driver of electricity. The model used in this paper is based on [13]. The model creates synthetic occupancy data based on a first order *Markov-Chain*, this is a well-proven and used technique. The model requires the deduction of a *Transition Probability Matrix* (TPM), and this is calculated from a source data; that details the probability of a transition from one level of active occupancy to another, at each time step throughout a day. For simplicity, this paper uses data obtained from the *Time Use Survey* (TUS) [13], this data has been used in several publications with extremely good results.

B. *Individual Appliances Model*

Model of individual appliances is used to simulate the use of all the major types of domestic electrical appliances, including (i) cold, (ii) cooking, and (iii) wet categories. The model uses individual appliances demand based upon activity

profiles, constructed from time use data, which represents how people spend their time. Finally, the model sums the electrical demand of each appliance at a given time providing the aggregate demand of the DC-house. An implementation of the individual appliance model is available in the form of Microsoft Excel Sheet at https://dspace.lboro.ac.uk/2134/8774, it includes activity profiles and other relevant data. The authors of this paper have created a MATLAB implementation of this code including and Microsoft Excel interface.

C. PV Generation Model

The photovoltaic generation model is based on two components: (i) *irradiance model* and (ii) *PV production model*.

Irradiance Model: The level of outdoor irradiance at calculated as the produce of two main aspects: (a) *Model of irradiance at the surface during 'clear sky' conditions.* The clear sky irradiance, at a specific point (longitude and latitude), can be approximated by the calculation of the solar position. In this paper, *Haurwitz clear sky model* for *global horizontal irradiance* (GHI) as presented [17]. (b) *Model of irradiance attenuation.* This attenuation is a consequence of the changing weather conditions; it is particularly relevant in the case of clouds passing overhead throughout the day. Detailed modelling of patching clouds moving across the sky using detailed atmospheric model requires complex processes. The data of the attenuation caused by cloud can be approximated using synthetic data. A simple way to model irradiance attenuation is using a clearness index. Synthetic data of clearness index is created using a first order Markov-Chain; this is a well-proven and used technique. The *Transition Probability Matrix* (TPM) used in this paper is based on [16].

PV production Model: A simple conversion model is used for the PV production chain. The model requires the incident radiation at the PV panel location; it uses the surface area of the panel array, and a global general efficiency to calculate the generated power. This approach has been used in the literature with extremely good results.

D. Wind Turbine Model

A simple energy conversion model is used for the wind turbine. The wind turbine generator is modelled such that the electrical power is the product of a system efficiency and the wind power incident on turbine blade (P_{wind}) is:

$$P_{wind} = \frac{1}{2} C_p \rho \pi R^2 w_w^3 \tag{1}$$

where, C_p is a power coefficient ρ is the air density (1.225 kg/m^3), R is the blade length (m) and v_w is the wind speed.

E. Battery Energy Storage System (BESS)

During the BESS charging/discharge process, the available power from BESS can be expressed as (lossless power converter):

$$P_{BESS} = \min\left\{P_{\max}, \max\left[0, \frac{SOC(t) - SOC_{\min}}{\Delta t}\right]\right\} \tag{2}$$

where P_{BESS} represents the rate of charge of BESS, it depends on the *state of charge* (SOC), and the *rated charging power*, P_{max}.The SOC in the BESS can be expressed as

$$SOC(t\Delta + t) = (1-\Theta)SOC(t) - \eta_{batt} P_{BESS}(t)\Delta t \tag{3}$$

where Θ is the self-discharge coefficient, η_{batt} is the efficiency during charging and discharging, and Δt is the time step.

IV. DC Power Flow Interactions

The classical load flow formulation considers the network under a single set of operating conditions. However, the classical load flow approach is unsuitable to the smart multi-terminal DC micro-grid (sMTdc) concept, because it includes the integration of renewable energy sources, time dependent demand with daily variations, and the complexity of the energy balancing process on off-grid networks using BESS. In this paper, a reasonable and pragmatic approach to simulate so-called "*Quasi-dynamic*" simulation is used. It consists of using a series of optimal power flow calculations and built-in parameter dependence on time.

In this paper the *Optimal power flow* (OPF) presented in [18] has been extended to simulate the time dependence of the RES, load demand and state of change of the BESS. The steady-state behaviour of a smart multi-terminal DC micro-grid (sMTdc) system is expressed by the nonlinear set of the algebraic equations [19] representing the power-balance across the system:

$$\mathbf{G}(\mathbf{X}, \mathbf{Y}) = \mathbf{0} \tag{4}$$

where $\mathbf{G}$ is the set of algebraic equations define the power balance at network buses as shown in (5), and $\mathbf{X}$ is *state vector* and $\mathbf{Y}$ is the *vector of the independent* variable. The state vector contains the state variables describing the state of the MTDC system, it contains *dependent variables* [20]. DC voltages can be dependent or independent variables depending on the voltage control used. Slack node and other voltage-type nodes provide known or independent variables contained in $\mathbf{Y}$. The OPF is formulated mathematically as [18, 20]:

$$\min f(\mathbf{X}, \mathbf{Y}) \tag{5}$$

Subject to:

$$\mathbf{G}(\mathbf{X}, \mathbf{Y}) = 0 \tag{6}$$

where $f(\mathbf{X},\mathbf{Y})$ is the function to be optimized. In this paper the objective function is used to minimize the total power losses (P_{losses}) as is applied on [21], [22], etc.:

$$f(\mathbf{X}, \mathbf{Y}) = P_{losses} = \sum_{i=1}^{n_{dc}} P_{dc,i} \tag{7}$$

where $P_{dc,i}$ are the elements in $\mathbf{P_{dc}}$ calculated in terms of the nodal voltages. An energy/power management system is expected to be part of sMTdc, it controls and monitors the operation of the sMTdc involving one or several DC-Houses, as consequence minimize the system losses is expected to be one of the sets of priorities during the normal and optimal steady-state operation [20].

DC/DC converters are used to control DC voltage inside MTDC. Limits are defined with regard to steady state voltage ranges at the converter stations. In this paper, the *i*-th node DC-voltage at power converter ($U_{dc,i}$) are written as bound constraints based on operational limits:

$$U_{\min} < U_{dc,i} < U_{\max} \tag{8}$$

where U_{min} and U_{max} represent the minimum and maximum allowed voltage.

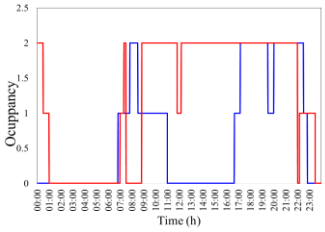
There is a very strict current limitation on the DC/DC converter used in MTDC systems. Using the nodal analysis, the nodal current can be transformed into a set of linear inequalities constraints as follow:

$$\mathbf{I_{conv}} = \mathbf{Y_{dc}}\mathbf{U_{dc}} < \mathbf{I_{conv}^{max}} \tag{9}$$

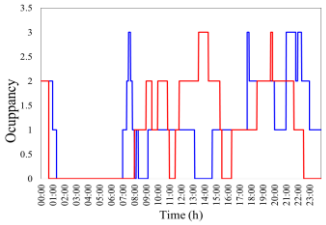
where $\mathbf{A_{ieq}} = \mathbf{Y_{dc}}$, $\mathbf{X} = \mathbf{U_{dc}}$.

V. Simulation and Results

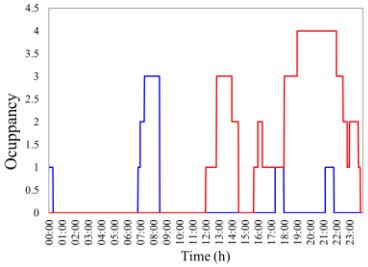
This section is dedicated to presents performance of a illustrate case of sMTdc, considering a set of three DC-Houses (*DC-House1*, *DCHouse2*, and *DC-House3*) are interconnected using a DC micro-grid in a star topology (data taken from [2]). The high-resolution (1-minute) demand of each DC-House is created considering a set of a number of residents, weekday and weekend days. The occupancy pattern is created considering the number of residents is assumed different in those houses and using the occupancy model presented in Section III. The results of the simulated active occupancy patterns are shown in Fig. 4.



(a) *DC-House1*: 2



(b) *DC-House2*: 3

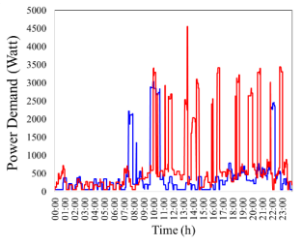


(c) *DC-House3*: 4

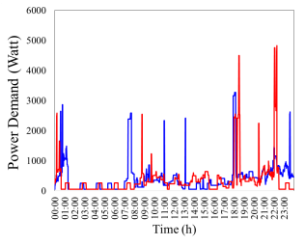
Fig. 4. Simulated Active Occupancy Pattern. Number of Residents presented in parenthesis.

Fig. 5 shows the simulated high-resolution electricity demand pattern for the three DC-houses (blue colour represents weekdays 'wd', and red colour weekends –'we'). Three global irradiances are simulated using the irradiance model presented in Section IIII. The simulated global irradiance pattern, including the cloud attenuation (see Fig. 6), is used to simulate the photovoltaic generation installed at each DC-House. A synthetic wind speed time series is created and then is introduced to the wind turbine model as presented in the previous section. A 2,000-Watt wind turbine is installed in *DC-House1* (see Fig. 7) .

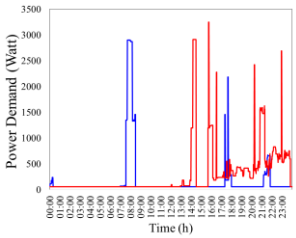
A MATLAB® R2015a (version 8.5.197613 64-bit) program (m-file) has been developed in order to illustrate the performance of the sMTdc presented above. All simulations are performed using a PC based on Intel®, Core™ i7 CPU 2.5GHz, 16 GB RAM with Windows 8.1 64-bit operating system.



(a) *DC-House1:* (436.94/711.60)



(b) *DC-House2:* (416.24/365.44)



(c) *DC-House3:* (165.19/290.32)

Fig. 5. Simulated Electricity Demand Pattern. Values presented in parenthesis represent averages values of weekday and weekend ('wd'/'we').

Fig. 5 shows the simulation results of DC-voltage in the three DC-Houses. The voltage profiles show an important dependence on the generation/demand balance in the sMTdc. *DC-Home1* has installed a wind turbine and a battery energy storage; therefore, the lowest voltage variations are reasonably located at *DC-House1*. The lower voltage profile in the sMTdc during weekends ('we'); this is a just consequence of the larger power consumption because of larger occupancy.

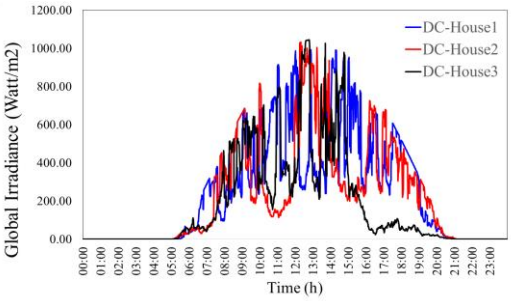


Fig. 6. Simulated Global irradiance considering attenuation due to clouds.

Fig. 8 shows the total losses in the sMTdc, considering load profiles for weekday and weekends, the maximum losses are related to weekend days when the demand is increased by the larger activity of home residents. Fig 9 shows the 24-hour evolution of the state of charge at the community battery energy storage system. It must me noticed how the SOC change during the day, decreasing and increasing. Special

mention deserves the increase of the SOC during late hours in the night when the load is low and there is high wind speed.

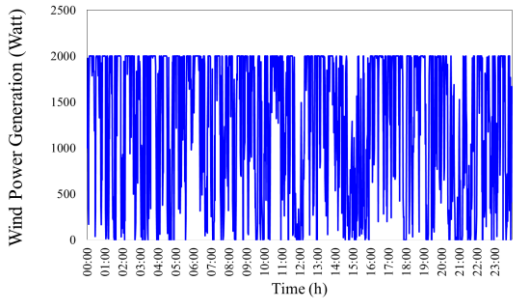
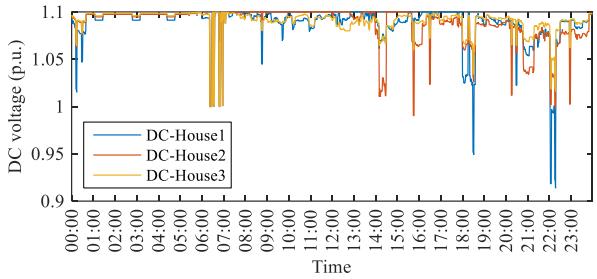


Fig. 7. Simulated Global irradiance with cloud attenuation.



(a) Weekdays ('wd')



(b) Weekend ('we')

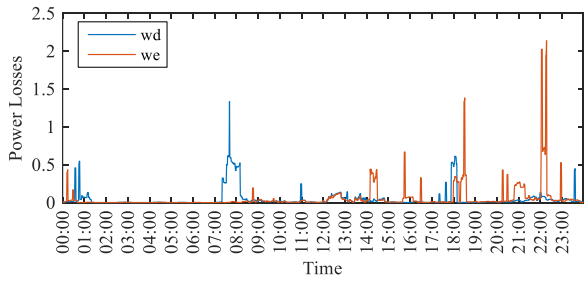


Fig. 8. Simulated Results: Power Losses (p.u).

VI. CONCLUSIONS

This paper presents a compressive introduction to the development of a simulation platform for smart multi-terminal DC micro-grid, this tool will facilitate the development of DC network to support a low-carbon sustainable electricity supply system. The simulation platform has been used to evaluate the appropriate performance of an illustrative/demonstrative sMTdc based on 3 DC-Houses. Each DC-House has a photovoltaic system, a wind turbine is included in the sMTdc and community battery energy storage system is using for balancing purposes. A Quasi-dynamic simulation approach using optimal power flow to minimize the system loads is used to obtain the voltage profile, power losses and state of charge of the BESS.

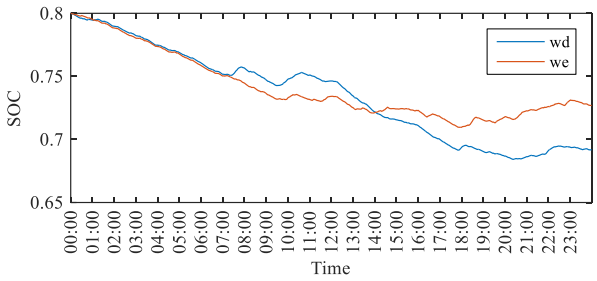


Fig. 9. Simulated Results: State of Charge (-).

REFERENCES

[1] F. Gonzalez-Longatt, "Frequency Control and Inertial Response Schemes for the Future Power Networks," in *Large Scale Renewable Power Generation*, J. Hossain and A. Mahmud, Eds., ed: Springer Singapore, 2014, pp. 193-231.

[2] F. Gonzalez-Longatt, B.S. Rajpurohit, and S. N. Singh, "Optimal Structure of a Smart DC micro-grid for a Cluster of Zero Net Energy Buildings," presented at the IEEE EnergyCon 2016, Leuven, Belgium, 2016.

[3] COOPERaTE. (2013). *COOPERaTE: Control and Optimization for Energy Positive Neighbourhoods*. Available: http://www.cooperate-fp7.eu/index.php/home.html

[4] DIMMER. (2013). *DIMMER: District Information Modeling and Management for Energy Reduction*. Available: http://dimmer.polito.it/

[5] EPBD. (2014). *Towards 2020 – Nearly Zero Energy Buildings*. Available: http://www.epbd-ca.eu/themes/nearly-zero-energy

[6] MESMERISE-CCS. (2014). *MESMERISE-CCS: Multi-Scale Energy Systems Modelling Encompassing Renewable, Intermittent, Stored Energy And Carbon Capture And Storage* Available: https://ukccsrc.ac.uk/resources/ccs-projects-directory/multi-scale-energy-systems-modelling-encompassing-renewable

[7] SHINE-ZC. (2011). *SHINE-ZC: Sustainable Housing Innovation Network of Excellence - Zero Carbon*. Available: http://gtr.rcuk.ac.uk/project/DB712AB2-B58A-4947-AB0C-C890F2BB1BCB

[8] ZenN. (2013). *ZenN : Zero Energy Building Renovation*. Available: http://www.zenn-fp7.eu/

[9] (2016). *Smart Multi-Terminal DC m-grids for autonomous Zero-Net-Energy Buildings*. Available: http://mtdc4zneb.org/

[10] F. Gonzalez-Longatt, B. S. Rajpurohit, and S. N. Singh, "Smart Multi-Terminal DC micro-grids for Autonomous Zero-Net-Energy Buildings: Implicit Concepts " presented at the IEEE PES Innovative Smart Grid Technologies 2015 Asia, ISGT Asia 2015, Bangkok, Thailand, 2015.

[11] B. S. R. K. Chauhan, R. E. Hebner, S. N. Singh, F. Gonzalez-Longatt, "Voltage Standardization of DC Distribution System for Residential Buildings," *Journal of Clean Energy Technologies*, vol. 4, pp. 167-172, 2016.

[12] G. Pandey, S. N. Singh, B. S. Rajpurohit, and F. M. Gonzalez-Longatt, "Smart DC Grid for Autonomous Zero Net Electric Energy of Cluster of Buildings," *IFAC-PapersOnLine*, vol. 48, pp. 108-113, // 2015.

[13] I. Richardson;, M. Thomson;, and D. Infield, "A high-resolution domestic building occupancy model for energy demand simulations," *Energy and Buildings*, vol. 40, pp. 1560–1566, 2008.

[14] I. Richardson, M. Thomson, D. Infield, and C. Clifford, "Domestic electricity use: A high-resolution energy demand model," *Energy and Buildings*, vol. 42, pp. 1878-1887, 10// 2010.

[15] I. Richardson, M. Thomson, D. Infield, and A. Delahunty, "Domestic lighting: A high-resolution energy demand model," *Energy and Buildings*, vol. 41, pp. 781-789, 7// 2009.

[16] I. Richardson and M. Thomson, "Integrated simulation of photovoltaic micro-generation and domestic electricity demand: a one-minute

resolution open-source model," *Proceedings of the Institution of Mechanical Engineers, Part A: Journal of Power and Energy*, vol. 127, pp. 73-81, 2012.
[17] B. Haurwitz, "Insolation in relation to cloudiness and cloud density," *Journal of Meteorology*, vol. 2, pp. 154-166, 1945/09/01 1945.
[18] F. Gonzalez-Longatt, "Optimal Power Flow in Multi-terminal HVDC Networks for DC-System Operator: Constant Current Operation," presented at the 50th International Universities Power Engineering Conference (UPEC 2015), Stoke-on-Trent, 2015.
[19] F. Gonzalez-Longatt, "Optimal power flow in MTDC systems based on a DC-independent system operator objective," in *PowerTech, 2015 IEEE Eindhoven*, 2015, pp. 1-6.
[20] F. Gonzalez-Longatt, "Optimal Steady-State Operation of a MTDC system based on DC-Independent System Operator Objectives," in *AC and DC Power Transmission, 11th IET International Conference on*, 2015, pp. 1-7.
[21] M. Aragüés-Peñalba, A. Egea-Àlvarez, O. Gomis-Bellmunt, and A. Sumper, "Optimum voltage control for loss minimization in HVDC multi-terminal transmission systems for large offshore wind farms," *Electric Power Systems Research*, vol. 89, pp. 54-63, 8// 2012.
[22] R. T. Pinto, P. Bauer, S. F. Rodrigues, E. J. Wiggelinkhuizen, J. Pierik, and B. Ferreira, "A Novel Distributed Direct-Voltage Control Strategy for Grid Integration of Offshore Wind Energy Systems Through MTDC Network," *Industrial Electronics, IEEE Transactions on*, vol. 60, pp. 2429-2441, 2013.